Static and Dynamic Nonlinear Effects in Silicon Micro-Rings: Impact of Trap Assisted Shockley Read Hall Carrier Recombination

(Article begins on next page)

16 July 2022

INTRODUCTION

It is well known that silicon waveguides and rings experiment important non-linear effects that often hinder the use of these devices in silicon photonic integrated circuits dealing with power in the order of a few tens of milliwatts. This is in particularly true in ring resonators, where high circulating power can be reached. As a result, in order to efficiently design silicon based micro-ring resonator, an accurate model is needed. Models in the literature, developed to fit experiments, are based on empirical expressions for the carrier lifetime[1],[2] and thermodynamic modelling of self-heating [3]. We present a new model that is based on the Shockley-Read-Hall (SRH) theory to predict the carrier lifetime of free carriers (FC) generated in the silicon waveguide core. We show that, by properly defining values for the energy of traps and surface trap density, we are able to reproduce experimental measurements in both steady state and in time domain when the ring output power presents periodic oscillation even with CW injection. This oscillating regime is due to the interplay between FC generation and self-heating. We also propose pump-probe experiments for measuring the time evolution of the ring transmission spectrum and then retrieve the time recovery of the non-linear absorption and refractive index change.

MODEL

Our theory is based on the well-established model of Two Photon Absorption (TPA), Free Carrier Absorption (FCA), Free Carrier Dispersion (FCD) and self-heating [2] in silicon. The inclusion of the SRH non radiative recombination of the free carriers is performed with the introduction of the rate equations for trap assisted recombination processes [4] which allows us to calculate the excess electron (n_e) and hole (p_e) generated by TPA. The electron and holes SRH rate equations can be decoupled in steady state making it possible to solve them analytically. The self-heating is included by calculating the temperature increase due to the power absorbed in the silicon core. For fixed input bus power P_{bus} and wavelength λ_{in} we solve a non-linear system that returns the power circulating in the ring (P_c), the excess carriers, the effective waveguide loss, the variation of refractive index and the temperature increase. Sweeping λ_{in}, we can then compute the transmission coefficient of the ring and compare it with the experiments. To simulate the ring dynamics and oscillating behaviour, the model is also extended to the time domain by naturally solving the SRH rate equations coupled with the dynamic equation for the circulating optical electric field in the ring. In this framework the temperature variation in time is modelled in Comsol Multiphysics and thermal time constants are derived in accord with [3]. This model can be also used to interpret the and probe experiments discussed in the following.

RESULTS

We consider a racetrack ring of total length of $80 \ \mu m$. The ring waveguide has a width of $W = 450 \ nm$ and height $h = 215 \ nm$. Steady state measurements were performed by a forward wavelength sweep from blue to red around

a selected cold resonance wavelength $\lambda_0 \approx 1540.2\ nm$ using an Agilent 8168A and a N7714A tunable lasers. The measured spectra were then fitted with the theoretical model to reproduce the shift of resonant wavelength and the variation of the transmission coefficient at resonance as a function of P_{bus}. The energy level of traps E_t and the related surface trap densities were set as the fitting parameters, the first was varied around the middle of the band gap while the second is expected to be in the range $10^{10} - 10^{12}\ cm^{-2}$ [5]. Fig. 1 (a) and (b) shows the fitting results in the case $E_t = 0.69\ eV$, $N_s = 7.4 \cdot 10^{10} cm^{-2}$. Fig. 1(c) reports the comparison between measured and simulated transmission spectra at low input power (almost linear regime) and high power when strong non-linear effects and self-heating are excited. The larger error bars in Fig. 1(a) and (b) refers to the precision of the high power tunable laser employed in measurements, whereas the error bar in Fig. 1(c) refers to output power oscillations observed at high input power.
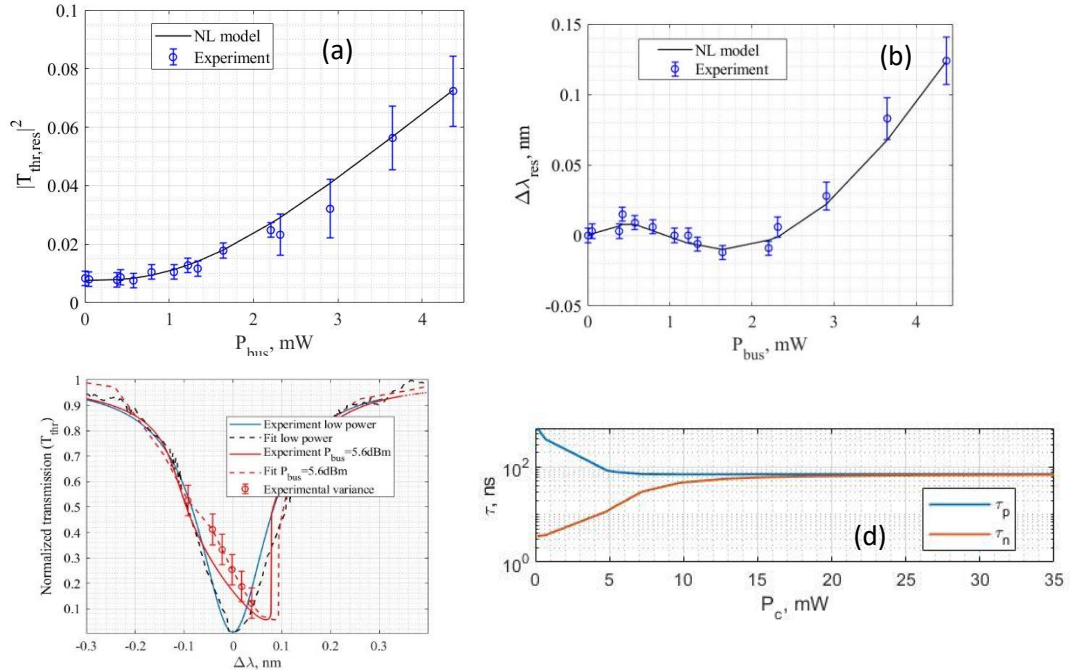

Fig. 1. Shift of resonant frequency (a) and variation of transmission at the through port at resonance (b), blue dots represent values extracted from measured spectra. From the fitting procedure we have $E_t = 0.65\ eV$, $N_s = 5.7 \cdot 10^{10} cm^{-2}$. (c) Low power (blue) and high power (red) transmission coefficient, dashed line are measured transmission coefficients, the red error bar indicate the oscillatory behaviour caused by the interplay of FC and self-heating with CW input power . (d) Holes and electron lifetime as a function of the calculated circulating power.

Fig. 1 (d) shows the calculated hole and electron lifetimes, defined as $\tau_{p,n} = \frac{(n_e, p_e)}{G_{TPA}}$, as a function of P_C. Both lifetimes exhibit a non linear behaviour because they are function of the circulating power and this dependence is essential to reproduce the experimental results. We note that for bus power higher than $1.5\ mW$, corresponding to $P_c = 15\ mW$, both holes and electrons lifetime tend to a costant value equal to $\tau_\infty \approx 70\ ns$, meaning that all traps are saturated by captured carriers. In this case electrons and holes dynamics can be approximated as equal, which justifies the assumption considered in other works [1,2,3]. Nonetheless thanks to our SRH model we can calculate the lifetimes without the need of any empirical expression. With the fitting parameters retrieved from the steady state analysis and measurements, we proceeded in reproducing periodic oscillations of the ring observed by measuring the time trace of the output power at the through port of the racetrack resonator. Fig. 2 (a) shows the superposition of the normalised output signal recorded with an oscilloscope and the prediction from the model in the time domain when we inject CW $P_{bus} \approx 11\ dBm$ at $\lambda_{in} \approx \lambda_0$. We can see that the model is able to follow the measured signal very well and can predict the periodicity of the oscillations. By analysing the simulated time evolution of excess carriers and circulating power in Fig. 2(b) and the variation of effective refractive index due to FCD and self-heating in Fig. 2(c) we are able to explain the origin of these self-oscillations as the interplay between the FC dynamics and the thermal transient which causes the resonant wavelength to oscillate with time (blue curve in Fig. 3c). We conclude by proposing a pump-probe experiment whose principal steps are summarised in Fig. 4. We set an high energy pulsed pump signal ($P_{pump}(t)$) with pulse width equal to $200\ ps$ and a period of $130\ \mu s$ at a

ring resonance $\lambda_{0,pump} = 1547.1\ nm$, whereas the CW probe wavelength λ_{probe} is swept around the cold nearest resonance at $\lambda_{0,probe} = 1540.2\ nm$, as sketched in Fig. 4 (a).
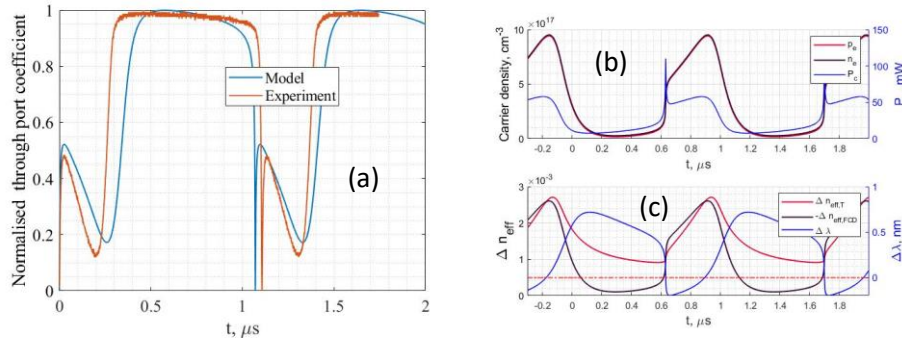

Fig. 3. (a) superposition of the normalized through port signal recorded on an oscilloscope and simulated through port coefficient for (b) Simulated holes and electron carrier densities (left) and circulating power (right) as a function of time. (c) Variation of refractive index due to temperature and FCD (left) and resonant wavelength (right) in time.

Generated free carriers by the pump pulse force a refractive index change that causes a blue shift of the resonance. The variation of the probe power depends therefore on the relative position of λ_{probe} with respect to the cold resonance wavelength $\lambda_{0,probe}$. By recording many different pump traces at different wavelengths λ_{probe}, we can reconstruct the ring spectral response at different time instants after the pump pulse. By fitting the time resolved transmission spectra we can extract the variation of effective refractive index due to FCD ($\Delta n_{eff,FCD}$) and the nonlinear loss as a function of time as shown in Fig. 4(e). The model we developed will then be applied to understand these recovery dynamics.
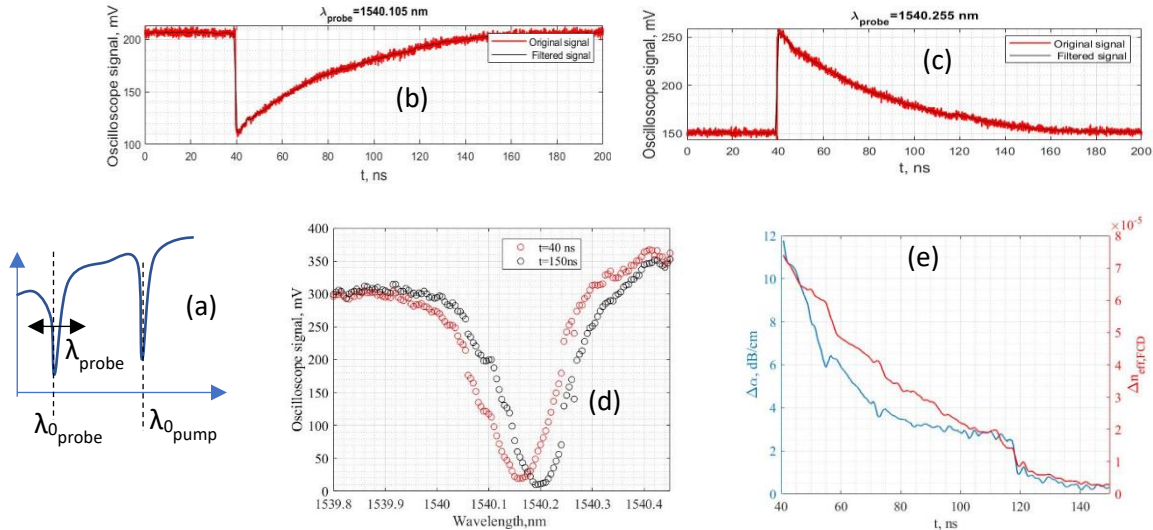

Fig. 4. (a) Schematic of the pump-probe experiment. (b) and (c) show probe powers traces signals recorded at the oscilloscope at the through port for probe wavelength below (b) and above (c) the cold resonance. (d) Time resolved spectral response of the ring around $\lambda_{0,probe}$ at $t = 40ns$ (just after the pump pulse) and at $t = 150ns$ (when the non-linear transient is concluded and the ring is in linear regime). (e) Extracted variation of effective refractive index due to FCD and non-linear loss in the ring versus time.

References

[1] P. E. Barclay, K. Srinivasan, and O. Painter, "*Nonlinear response of silicon photonic crystal microresonators excitedvia an integrated waveguide and fiber taper*," Opt. Express13, 801–820 (2005).
[2] G. Priem, P. Dumon, W. Bogaerts, D. V. Thourhout, G. Morthier, and R. Baets, "*Optical bistability and pulsatingbehaviour in silicon-on-insulator ring resonator structures*." Opt. Express13, 9623–9628 (2005)
[3] M. Borghi, D. Bazzanella, M. Mancinelli, and L. Pavesi, "*On the modeling of thermal and free carrier nonlinearitiesin silicon-on-insulator microring resonators*," Opt. Express29, 4363–4377 (2021)
[4] J. Blakemore,*Semiconductor Statistics*, Dover Books on Physics Series (Dover, 2002).